Cathodic Contact Glow Discharge Electrolysis for the Degradation of Liquid Ammonia Solutions

Anis Allagui,* Nicolas Brazeau, Hussain Alawadhi, Fares Al-momani, Elena A. Baranova

The application of 50 VDC cathodic contact glow discharge electrolysis for six hours in 1.0 mol/L KOH + 0.8, 0.4 and 0.08 g/L ammonia results in the removal of 66, 71 and 77% of ammonia, respectively, following pseudo first-order kinetics at ca. 0.3 mol/kWh. The yields of dissolved NO_2—N and NO_3—N lie between 9 and 29% and are coupled with ammonia removal suggesting a nitrification process. Based on the near-cathode UV–Vis emissions and ionization products of H_2O and NH_3 molecules, a mechanism is proposed along with the charge/energy transfer reactions between the plasma-generated free radicals and ionic species. Joule heating and vaporization are also believed to physically remove ammonia.

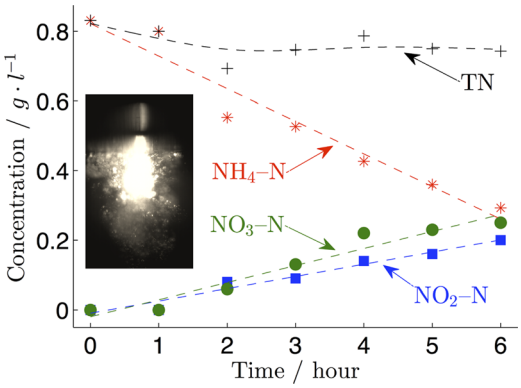

1. Introduction

In contrast to low-current density electrochemistry, when the terminal voltage in a two-electrode cell is higher than a critical value (Figure 1d), one can observe a transition from conventional electrolysis (Figure 1a–c) to the emission of visible light (Figure 1e–g) from the submerged active electrode. Current flows through a dielectric gaseous envelope formed around the electrode as glow micro-discharges. In this instance, the intermittent electrical discharges are the source of free radicals and chemically active species, such as H·, OH·, and H_2O_2 at remarkably non-faradaic yields.[1–5] The physicochemical properties of contact glow discharge electrolysis (CGDE) have been adapted to a multitude of applications such as synthetic chemistry,[6–8] micrometer-precision machining of non-conductive materials,[9,10] and more recently to nanoparticles synthesis.[11–14] Non-equilibrium atmospheric pressure discharges, also known as non-thermal plasmas, electrochemical discharges, atmospheric plasma jet or corona discharges have also been successfully used for bio-decontamination, sterilization, and purification of water streams from organic dyes, phenols, and organic halides.[15–20] Treatment of inorganic materials by non-thermal plasma processes have not received the same attention in the literature, and has mostly focused on the oxidation and removal of chromium (VI).[21,22] The mechanism of plasma oxidation relies mainly on the powerful oxidizers generated by the process, such as the hydroxyl radical, atomic oxygen, electronically excited oxygen, ozone, etc.

Dr. A. Allagui
Sustainable and Renewable Energy Engineering, University of Sharjah, 27272, Sharjah, United Arab Emirates
E-mail: aallagui@sharjah.ac.ae
N. Brazeau, Dr. F. Al-momani, Dr. E. A. Baranova
Department of Chemical & Biological Engineering, University of Ottawa, 161 Louis-Pasteur, Ottawa, ON, Canada K1N 6N5
Dr. H. Alawadhi
Department of Applied Physics, University of Sharjah, 27272, Sharjah, United Arab Emirates

DOI: 10.1002/ppap.201400049

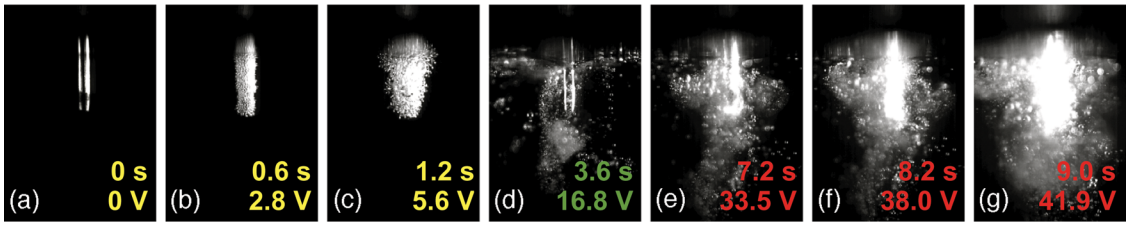

Figure 1. From conventional electrolysis to contact glow discharge electrolysis (a–g): 0–45 VDC linear scan at 4.65 V/s around a 0.5 mm Ni cathode in 6 mol/L KOH solution, acquired with a PC-controlled Phantom V 9.1 high resolution high speed camera (1 000, 14-bit depth, frames per second at 1 632 × 1 200 px full resolution) preset at 83 frames per second and an exposure time of 1 ms. Three LED lamps mounted in T-configuration were used to illuminate the Ni wire.

Ammonia has been a real concern for decades, and a number of techniques have been developed to degrade this compound in waste streams. Some of the conventional strategies for ammonia degradation are air stripping, breakpoint chlorination, ion exchange, use of zeolites, biological nitrification/denitrification, ozonation, and photo-catalytic oxidation. More recently, electrochemical oxidation has shown promising results for ammonia removal at low concentrations.[23–25] Each of these methods has its own pros and cons that are mainly related to the initial or operating costs of the procedure, the efficiency of ammonia removal, and the possible generation of secondary non-desirable wastes. Comparative studies of these techniques can be found in the reviews of Kapoor and Viraraghavan[26] and Mook et al.[27]

Although studies of glow discharges in liquid ammonia solutions or in ammonia-gas mixtures have been reported,[28–32] they have usually been conducted at high applied voltages and without proper investigation of its degradation kinetics. The aim of the present work is to investigate the simple, compact, and straightforward process of cathodic CGDE in dissolved ammonia in highly conductive KOH solution, allowing the process to ignite at low DC voltages. Time-current discharge activity, current–voltage characteristics and near-cathode emission spectroscopy in the 300–850 nm wavelength range are used to describe the electrical and spectrochemical properties of cathodic CGDE in liquid ammonia solutions.

2. Experimental Section

Investigations of cathodic CGDE were carried out in 150 ml aqueous solution of 1.0 mol/L KOH + c (c = 0.8, 0.4, and 0.08) g/L of ammonia (NH_4OH 14.8 N, Fischer Scientific) poured in a two-compartment cell separated by a glass frit. The centre-to-centre distance was 10 cm. A nickel wire (0.5 mm diamter, 99.99% purity, Advent Research Materials) slightly immersed into the solution with *ca.* 6.5 mm^2 surface area served as the cathode, while a large stainless steel coil of grade 304 was used as the anode. Solutions in both compartments were under continuous gentle stirring with magnetic bars. The terminal voltage was set to 50 VDC, supplied by a programmable switching DC power supply. The time-current signal was recorded using a current probe (Agilent, model N2774A-50 MHz) at a sampling rate of 10 kS/s. Optical emission spectroscopy, which is a simple and popular tool for plasma diagnostics providing information on species in electronic excited states, was acquired with an Ocean Optics HR2000 high-resolution spectrometer. The HR2000 has a 300 lines per mm diffraction grating, 10 μm entrance slit, a Sony ILX511 2048-Pixel element linear CCD array detector, and is operating in the effective wavelengths range 300–1 100 nm. The CCD integration time was set to 1 s and the recorded spectra were averaged over three readings to increase signal-to-noise ratio. The spectrometer is connected to an optical fiber P200-2-UV–VIS 2-m long, 200 μm core diameter, placed outside of the cell and pointing at the near-cathode (tungsten or nickel, 0.5 mm diameter, 99.99% purity) region. Background spectra of ambient emissions are collected at the beginning of each experiment and deducted from the spectra for all results presented in this work. Both ammonia-free and ammonia-containing KOH solutions were investigated by optical emission spectroscopy with reference to the NIST Atomic Spectra Database.[33]

Six-hour cathodic CGDE experiments were carried out in the three ammonia solutions (c = 0.8, 0.4, and 0.08 g/L). A 2 ml sample was collected hourly from the cathode compartment. Control samples were also taken and analyzed to correct the real ammonia removal values with the stripping amounts, which was found to not surpass 1%. Ammonia was measured according to Standard Methods, Method 4500–NH_3 B and C[34] using a HACH spectrophotometer (DR2000, HACH Company, USA) at 425 nm. Nitrite was measured according to the diazotization method using HACH powder pillows (Nitrite Method 8507) and HACH spectrophotometer at 505 nm. Nitrate was measured using HACH cadmium reduction method using HACH powder pillows (Nitrate Method 10020) and the spectrophotometer at 500 nm. Samples were analyzed three times with a reproducibility of ±0.1 mg-N/L. The reported concentration values in this work are averaged over the three measurements.

3. Results and Discussion

3.1. Electric Characteristics

A typical mean current–voltage curve in 1.0 mol/L KOH with the linear variation of the cell voltage from 0 to 55 V at 10 V/s is shown in Figure 2. Three different current

DOI: 10.1002/ppap.201400049

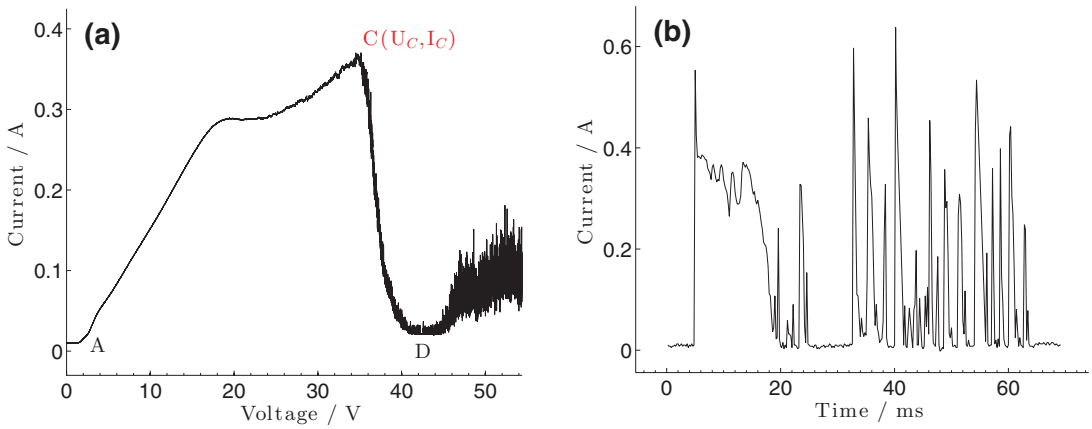

Figure 2. a) Mean current-voltage characteristics of cathodic contact glow discharge electrolysis and b) current time-series during the discharge activity at 50 VDC, in 1.0 mol/L KOH solution.

behaviors are identified. Region A–C shows first a quasi-linear increase of current with the voltage, where Ohm's law is satisfactorily obeyed and corresponding to the conventional electrolysis. It is then followed by a plateau due to the vigorous gas evolution and saturation of the electrode surface. The increase of voltage and the rise of the local temperature lead to the formation of a fully developed gas film covering the electrode and insulating it from the rest of the solution, followed by the abrupt current breakdown in the unstable region C–D (transition between Figure 1c and d). With further increase of the terminal voltage, starting from point D where the current and voltage readings are stabilized again, electrons emitted from the cathode are accelerated in the gas film and collectively initiate the discharge regime and the emission of visible light,[1] as shown in Figure 1e–g. The choice of 50 VDC terminal voltage for ammonia removal in this work ensures a safe distance from the instability region depicted in the current–voltage readings in Figure 2a.

A short 10 kS/s current time-series, collected during the discharge process in 1.0 mol/L KOH at 50 VDC, is shown in Figure 2b. The gas film formation response, which takes about 15 ms, is followed by high frequency pulses characterizing the discharge activity.[2,36] The average lifetime of a collective discharge is around 1 ms but it can be superposed by another discharging event occurring at another location of the active electrode,[10] as it can be seen in Figure 2b. The signal is stochastic, where both gas film formation, and discharges have irregular magnitudes, building times, and frequencies of appearance in the time–current response.[35] The system is self-maintaining, i.e., if the purely potential-dependent gas film breaks for whatever reason, there will be a fast surge in power to reform the gas film and re-establish the discharge regime again.

3.2. Optical Emission Spectroscopy

A typical time-integrated spectrum in the 300–850 nm wavelength range, collected near a tungsten wire in 1.0 mol/L KOH + 0.8 g/L ammonia at 50 VDC, is shown in Figure 3. The optical emission in ammonia-free KOH solution under the same conditions is measured as a reference, but is not shown here. The collection of time-series spectra show continuous time variations of the peak intensities due to the random duration and intensity of discharges (see Figure 2b). This is a consequence of the continuous change in local conditions of the system, such as the alternating formation and breaking of the gas film, the time/frequency characteristics of the discharges (see Figure 2b) and the electrode surface state.[35] The spectrum consists of strong lines with a weak continuum. The most

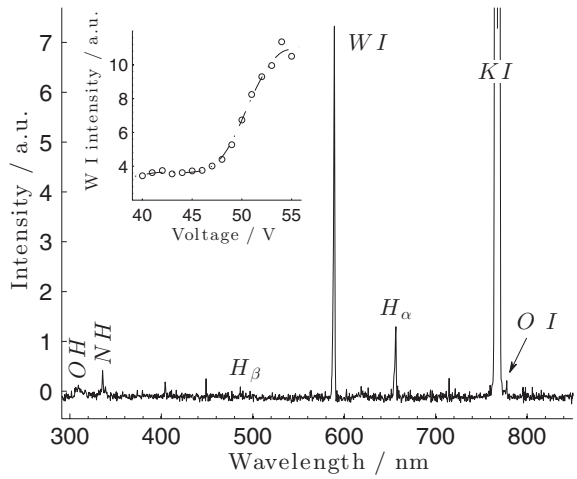

Figure 3. Optical emission spectrum collected near a tungsten cathode in 1.0 mol/L KOH + 0.8 g/L ammonia at 50 VDC. The insert shows the effect of applied voltage on the W I emission line intensity.

pronounced peaks correspond to the K I doublet atomic emissions lines at 766.6 and 770.1 nm, respectively, followed by the W I line at 589.2 nm. The appearance of W I lines indicates that the cathode electro-erosion or sputtering is a dominant process during cathodic CGDE.[11] Additionally, the intensity of the emission lines increases with the applied cell voltage, which in turns increases the mean current density (see Figure 2a beyond point D) and the conductivity of the plasma glow-discharge. The insert in Figure 3 clearly shows this effect for the atomic emission line W I at 589.2 nm. The same overall trend is recorded for other lines. In the visible range, we also observe the atomic hydrogen spectral lines of the Balmer series H_α at 656.5 nm, with a weak response from the second line H_β at 486.4 nm. The UV hydroxyl OH band centered at 309.3 nm, corresponding to the transition $A^2\Sigma^+ (=0) \rightarrow X^2 (\nu = 0)$, was also detected in the short wavelength spectral range. The small hump around 618.4 nm corresponds to the second order line of the OH radical emission at 309.3 nm.[36] The weak features corresponding to atomic O I lines at 777.2 ($3p\ ^5P^0 \rightarrow 3s\ ^5S^0$) and 844.7 nm ($3p\ ^3P^0 \rightarrow 3s\ ^3S^0$) are observed in the near-infrared region. All these emission lines were detected in both ammonia-containing and ammonia-free KOH solutions. The spectral lines are mainly sharp atomic lines originating from the surrounding aqueous electrolyte and the electrode material, with a few neutral molecular lines and no ionic lines. This is an indication that the plasma is cold.

With the addition of ammonia to the KOH solution, intensities of all emission lines decreased slightly due to the decrease of the electrical conductivity. The NH ($A^3\Pi$–$X^3\Sigma^-$) band is observed in the spectrum at 335.7 nm most probably due to the dissociation of ammonia molecules.

3.3. Chemical Analysis and Mechanism

Figure 4 shows the time-concentration profiles of NH_4-N, NO_2-N, NO_3-N, and Total Nitrogen (TN) during the ammonia degradation process by cathodic CGDE in 1.0 mol/L KOH + c ($c = 0.8$, 0.4, and 0.08) g/L ammonia. The concentration of NH_4-N in the first 0.8 g/L solution decreased by 66% by the end of the 6-h experiment (Figure 4a). The removal efficiency of ammonia–nitrogen, calculated as $100 \times \left(1 - [NH_4 - N]_{t+1}/[NH_4 - N]_t\right)$ where $t = 0, 1, \ldots, 5$ h, stabilized to about 18% in the second half of the experiment, values close to what has been reported with microhollow cathode discharge in atmospheric pressure NH3(6.25%)/Ar gas mixture.[32] In the same time, about 24% and 29% of the initial concentration of NH_4-N are recorded for NO_2-N and NO_3-N, respectively. Mass balance of total nitrogen along the 6-h experiment, being the sum of masses of ammonia and its degradation by-products, indicates that the removal process was achieved by oxidizing the compound to nitrite and nitrate. Similar trends are observed for ammonia,

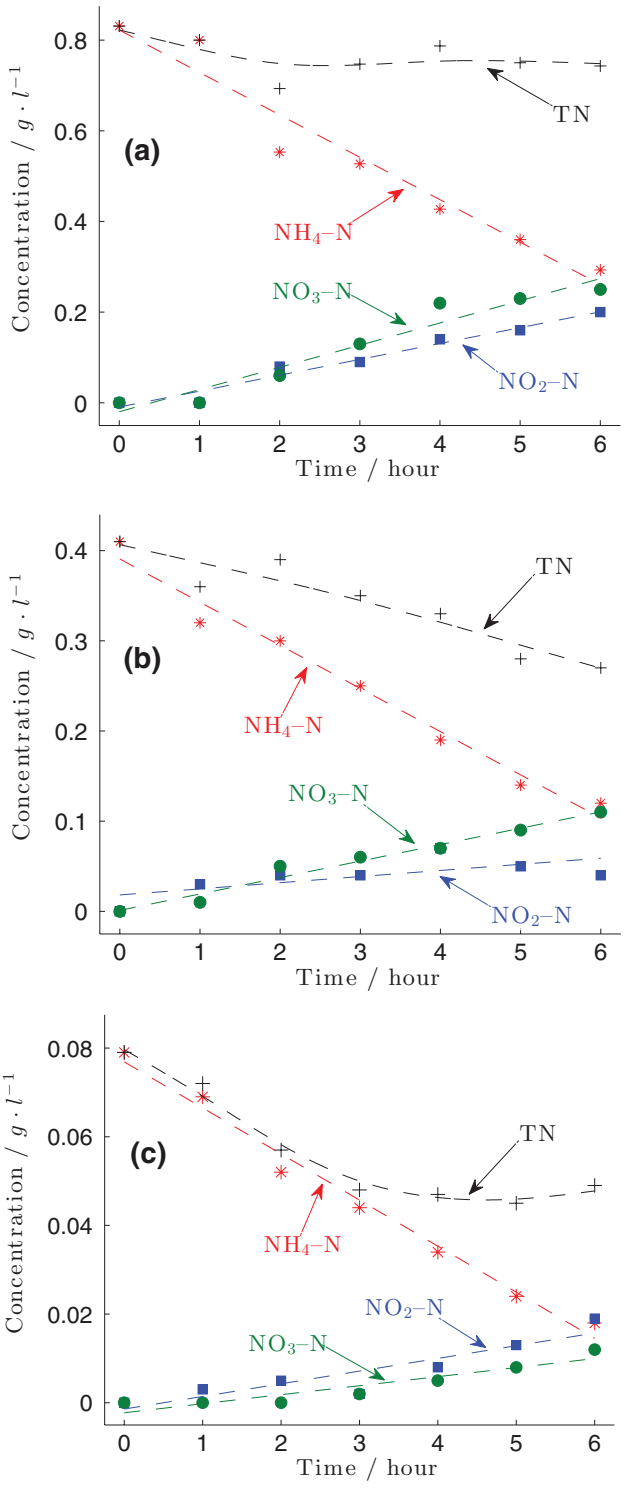

Figure 4. Normalized concentration profiles of NH_4-N, NO_2-N and, NO_3-N in 1.0 mol/L KOH + 0.8 a), 0.4 b), and 0.08 c) g/L of ammonia, during cathodic contact glow discharge electrolysis at 50 VDC.

Plasma Process. Polym. **2015,** *12*, 25–31

DOI: 10.1002/ppap.201400049

nitrite and nitrate concentrations plots from the other two solutions, as shown in Figure 4b and c, respectively. About 71% and 77% of ammonia were removed from the 0.4 and 0.08 g/L initial ammonia concentrations, respectively, with the generation of higher fractions of NO_3-N than NO_2-N compounds. The efficiency of NH_4-N degradation stabilized to 22% and 26%, respectively. With the decrease of the initial concentration of ammonia (0.4 and 0.08 g/L), the decline of TN with time indicates that other nitrogeneous species have been formed. Cathodic CGDE for the removal of liquid ammonia can be attributed in part to a nitrification process where the decrease of ammonia fraction is coupled with the increase of nitrate and nitrate concentrations. Figure 5 shows the linear time-decline of the logarithm of $[NH_4-N]_t$ normalized to the initial ammonia concentration $[NH_4-N]_0$, according to:

$$\log\left(\frac{[NH_4-N]_t}{[NH_4-N]_0}\right) = -kt \quad (1)$$

The process seems to obey pseudo first-order kinetics with constant rates equal to 0.18, 0.20, and 0.25 h^{-1} for the experiments with 0.8, 0.4, and 0.08 g/L initial ammonia concentration, respectively. The energy efficiency, estimated over the six-hour runs and average power of 2.5 W, is of the order of 1 μmol/J (0.3 mol/kW h) for the three ammonia solutions. However, using atmospheric pressure alternating current arc discharges for gaseous ammonia-to-hydrogen conversion, Zhao et al.[31] reported 12.5 mol/kW h energy efficiency making use of the high temperatures that can be attained within the reactor, while for microhollow cathode discharge experiments in NH_3 (6.25%)/Ar mixture, 1.3 mol/kW h was reported.[32] The energy efficiency in gaseous ammonia streams is higher than our results for liquid ammonia, which can be explained by the low residence time of ammonia molecules in the small plasma volume, as well as the continuous competition with other intermediaries and mass transport constraints.

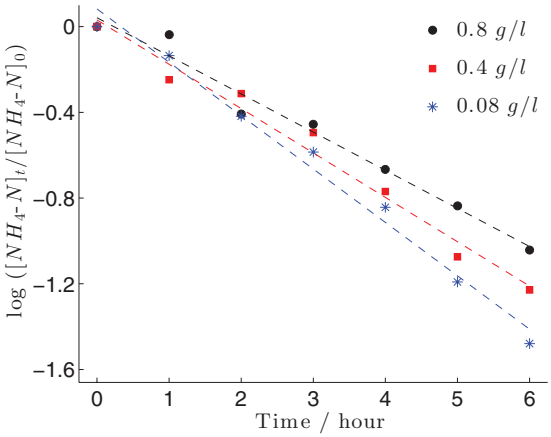

Figure 5. Time profile of the logarithm of $[NH_4-N]_t$ normalized to the initial 0.8, 0.4, and 0.08 g/L ammonia concentrations.

A plausible mechanism for cathodic CGDE in liquid ammonia solutions is proposed as follows. Hickling and Ingram[37] suggested for the anodic non-contact GDE—that has later been adapted by Senguta and Singh[3] for anodic CGDE—the mechanism in which the most probable charge carrier in the plasma channel is H_2O^+. This deduction was based on the work of Barton and Bartlett[38] and others, in which they showed the relative abundance of H_2O^+ ions produced by electron impact in water vapor. This mechanism involves the acceleration and impact of the charge carriers followed by diffusion in the primary and secondary reaction zones of the liquid surface, respectively. Because of the assumption of no important stopping power in the way of the charge carriers, an average of 100 eV energy was suggested for the H_2O^+ ions with a linear loss of about 100 eV/nm in the primary reaction zone. Ionization/activation by collision and charge transfer reactions can ultimately give H_2O_2, H_2, H·, and OH· radicals in the secondary reaction zone with possible recombination reactions with other elements present in the solution. The ionization potentials of water and ammonia by electron impact are 12.6 and 10.0 eV, respectively,[39] values exceeded by the electronic discharges process at 50 VDC in the innermost plasma volume.[40,29,32] On the other hand, results of mass spectrometry studies of ionized water vapor give:[41]

$$H_2O \rightsquigarrow e^-_{aq}, H^{\cdot}, OH^{\cdot}, H_2O^{\cdot}, H_2, H_2O_2, H_3O^+ \quad (2)$$

and for NH_3, the main species detected after dissociation are:[28,41–43]

$$NH_3 \rightsquigarrow e^-_{amm}, H^{\cdot}, NH_3^{\cdot}, NH_2^{\cdot}, NH^{\cdot}, H_2, N_2H_4, NH_4^+ \quad (3)$$

These species, generated by direct electron dissociation impact, are usually common in processes similar to CGDE, such as electron beam treatment and stream corona discharges.[44,45] Many charge transfer and energy transfer reactions are expected to occur with the generated active free radicals, ionic and molecular species at the vicinity of the glow discharges: direct electron impact dissociation, electron impact ionization/dissociative recombination, and ion-ion/molecule reaction/dissociative recombination.[4] In principle, with enough knowledge about the energy distribution functions of the different components of the glow discharges, it is possible to evaluate the relative rates of production/destruction of the different components of the supporting solution. To cite a few possible reactions, the dimerization and mixed reactions involving H·, OH· (observed in OES results of Figure 3) and $NH_2^{\cdot}$ radicals lead possibly to molecular species such as H_2, N_2H_4, NH_2OH and H_2O_2. The back reaction forming NH_3 involve the

recombination of H· and $NH_2^{\cdot}$, while water molecule is formed from the active species H· and OH·.[28,30] Gaseous N2 can arise from the secondary reactions $2N_2H_3 \rightarrow N_2 + 2NH_3$ and $2NH_2O \rightarrow N_2 + 2H_2O$.[30] Nitrite and nitrate may be formed due to the presence of oxygen radical and dissolved oxygen,[46,20] which is in accordance with the low intensities of their spectral lines in Figure 3, and the results in Figure 4.

In addition to the dissociation mechanism by impact of incident electronic discharges and oxidation of ammonia to nitrate and nitrite, it is worth mentioning that (i) increase of the local temperature around the cathode up to an average of 70° at 1 cm distance from the tip of the electrode, as well as (ii) vaporization of the electrolyte, enhanced by the convective bi-phasic flows, are believed to facilitate the removal of ammonia from the solution. Katehis et al. showed the gradual increase of ammonia removal by stripping/absorption process from ca. 35% at ambient temperature to 98% at 75°,[47] while Zhao et al.[31] reported a strong correlation between the increase of reactor temperature or electrode temperature with the increase of ammonia removal in AC arc discharge. On the other hand, the local generation of forced convective flow from the alternating gas film formation and breaking (see Figure 1e–f) is believed to physically removing ammonia by stripping process. Nonetheless, further studies are needed to understand the liquid ammonia degradation by this process and to elucidate the contribution of each of the different physicochemical properties of CGDE, such as simultaneous use of multiple sources of plasma micro-discharges, effect of the solution temperature, and applied cell voltage. Spectral emission measurements in the ultraviolet and infrared regions, and as a function of time may bring further insights into the mechanistic pathways of this process.

4. Conclusion

Solutions of 0.8, 0.4, and 0.08 g/L ammonia + 1.0 mol/L KOH under the impact of electronic discharges emitted during cathodic CGDE at 50 VDC are investigated. Ammonia decomposition at an average of 12% per hour is recorded for the three solutions, with pseudo first-order type kinetics. The generation of NO_2-N and NO_3-N are also recorded and do not exceed 30%, but are coupled with the degradation of ammonia suggesting a nitrification process. The electronic discharges emitted from the cathode surface brings in the necessary ionization energies of water and ammonia that dissociate these molecules to active radicals and ionic species such as H·, OH·, and $NH_2^{\cdot}$. By a series of primary and secondary charge transfer and energy transfer reactions, ammonia is transformed into NO_2, NO_3, H_2, and N_2, amongst other species. Further investigations are needed to control the nitrite and nitrate formation yields in order to consider the cathodic CGDE as an efficient process for ammonia removal from waste streams.

Acknowledgments: This work was supported by Fonds québécois de la recherche sur la nature et les technologies (Canada) and the University of Sharjah (United Arab Emirates) Project #140437. The authors are grateful to L. Chaabi, H. Bilal, and S. O. M. Oda for their assistance.

Received: April 6, 2014; Revised: July 4, 2014; Accepted: July 14, 2014; DOI: 10.1002/ppap.201400049

Keywords: ammonia; DC discharges; glow discharge; optical emission spectroscopy

[1] A. Hickling, M. D. Ingram, *Trans. Faraday Soc.* **1964**, *60*, 783.
[2] J. Garbarz-olivier, C. Guilpin, *J. Electroanal. Chem.* **1978**, *91*, 79.
[3] S. K. Sengupta, O. P. Singh, *J. Electroanal. Chem.* **1994**, *369*, 113.
[4] R. Akolkar, R. M. Sankaran, *J. Vac. Sci. Technol. A Vacuum Surf. Film* **2013**, *31*, 050811.
[5] J.-L. Brisset, D. Moussa, A. Doubla, E. Hnatiuc, B. Hnatiuc, G. Kamgang Youbi, J.-M. Herry, M. Natali, M.-N. Bellon-Fontaine, *Ind. Eng. Chem. Res.* **2008**, *47*, 5761.
[6] K. Harada, S. Suzuki, H. Ishida, *Biosystems* **1978**, *10*, 247.
[7] J. Gao, A. Wang, Y. Li, Y. Fu, J. Wu, Y. Wang, Y. Wang, *React. Funct. Polym.* **2008**, *68*, 1377.
[8] S. K. Sengupta, U. Sandhir, N. Misra, *J. Polym. Sci. Part A: Polym. Chem.* **2001**, *39*, 1584.
[9] R. Wüthrich, V. Fascio, *Int. J. Mach. Tools Manuf.* **2005**, *45*, 1095.
[10] R. Wüthrich, A. Allagui, *Electrolysis in Aqueous Solutions Under Extreme Current Densities—Fundaments and Applications of Electrochemical Discharge Phenomenon*, Nova Science Publishers Inc. **2010**.
[11] A. Allagui, E. A. Baranova, R. Wüthrich, *Electrochim. Acta* **2013**, *93*, 137.
[12] A. Allagui, R. Wüthrich, *Electrochim. Acta* **2011**, *58*, 12.
[13] D. Mariotti, R. M. Sankaran, *J. Phys. D. Appl. Phys.* **2010**, *43*, 323001.
[14] K. Ostrikov, *Rev. Mod. Phys.* **2005**, *77*, 489.
[15] P. Jamróz, K. Grda, P. Pohl, W. Zyrnicki, *Plasma Chem. Plasma Process.* **2013**, *34*, 25.
[16] X. Jin, H. Zhang, X. Wang, M. Zhou, *Electrochim. Acta* **2012**, *59*, 474.
[17] X. Wang, M. Zhou, X. Jin, *Electrochim. Acta* **2012**, *83*, 501.
[18] B. R. Locke, M. Sato, P. Sunka, M. R. Hoffmann, J.-S. Chang, *Ind. Eng. Chem. Res.* **2006**, *45*, 882.
[19] Y. J. Liu, X. Z. Jiang, *Environ. Sci. Technol.* **2005**, *39*, 8512.
[20] P. Lukes, E. Dolezalova, I. Sisrova, M. Clupek, *Plasma Sources Sci. Technol.* **2014**, *23*, 015019.
[21] L. Wang, X. Jiang, *Environ. Sci. Technol.* **2008**, *42*, 8492.
[22] Z. Ke, Q. Huang, H. Zhang, Z. Yu, *Environ. Sci. Technol.* **2011**, *45*, 7841.
[23] A. Allagui, M. Oudah, X. Tuaev, S. Ntais, F. Almomani, E. A. Baranova, *Int. J. Hydrogen Energy* **2013**, *38*, 2455.
[24] A. Allagui, S. Sarfraz, E. A. Baranova, *Electrochim. Acta* **2013**, *110*, 253.
[25] A. Allagui, S. Sarfraz, S. Ntais, F. A. momani, E. A. Baranova, *Int. J. Hydrogen Energy* **2014**, *39*, 41.
[26] A. Kapoor, T. Viraraghavan, *J. Environ. Eng.* **1997**, *123*, 371.

DOI: 10.1002/ppap.201400049

[27] W. T. Mook, M. H. Chakrabarti, M. K. Aroua, G. M. A. Khan, B. S. Ali, M. S. Islam, M. A. A. Hassan, *Desalination* **2012**, *285*, 1.
[28] A. Hickling, G. R. Newns, *J. Chem. Soc.* **1961**, 5177.
[29] A. Hickling, G. R. Newns, *J. Chem. Soc.* **1961**, 5186.
[30] G.-A. Mazzocchin, F. Magno, G. Bontempelli, *J. Electroanal. Chem. Interfacial Electrochem.* **1973**, *45*, 471.
[31] Y. Zhao, L. Wang, J. Zhang, H. Guo, *Int. J. Hydrogen Energy* **2014**, *39*, 7655.
[32] H. Qiu, K. Martus, W. Lee, K. Becker, *Int. J. Mass Spectrom.* **2004**, *233*, 19.
[33] R. Y. R. J. A. Kramida, N. A. Team, NIST Atomic Spectra Database (version 5.1). http://physics.nist.gov/asd.
[34] *Standard Methods for the Examination of Water and Wastewater* (Ed: A. E. Greenberg,) 16th ed., American Public Health Association, **1985**.
[35] A. Allagui, R. Wüthrich, *Electrochim. Acta* **2009**, *54*, 5336.
[36] B. Sun, M. Sato, J. S. Clements, *J. Electrost.* **1997**, *39*, 189.
[37] A. Hickling, M. Ingram, *J. Electroanal. Chem.* **1964**, *8*, 65.
[38] H. A. Barton, J. H. Bartlett, *Phys. Rev.* **1928**, *31*, 822.
[39] *CRC Handbook of Chemistry Physics* (Ed: David. R. Lide) CRC Press, Boca Raton, FL **2005**.
[40] R. M. Chaudrhi, M. L. Oliphant, *Proc. R. Soc. London Ser. A* **1932**, *137*, 662.
[41] M. M. Mann, A. Hustrulid, J. T. Tale, *Phys. Rev.* **1940**, *58*, 340.
[42] C. E. Melton, *J. Chem. Phys.* **1966**, *45*, 4414.
[43] B. Y. D. Cleaver, E. Collinson, F. S. Dainton, *Trans. Faraday Soc.* **1960**, *56*, 1640.
[44] A. A. Joshi, B. R. Locke, P. Arce, W. C. Finney, *J. Hazard. Mater.* **1995**, *41*, 3.
[45] Y. Mok, S. Ham, *Chem. Eng. Sci.* **1998**, *53*, 1667.
[46] P. Lukes, B. R. Locke, J.-L. Brisset, *Plasma Chem. Catalysis Gases Liquids* **2012**, 243.
[47] D. Katehis, V. Diyamandoglu, J. Fillos, *Water Environ. Res.* **1998**, *70*, 231.